

Phasic study of intestinal homeostasis disruption in experimental intestinal obstruction

Xiang-Yang Yu, Chang-Lin Zou, Zhen-Li Zhou, Tao Shan, Dong-Hua Li, Nai-Qiang Cui

Xiang-Yang Yu, Zhen-Li Zhou, Tao Shan, Department of Gastrointestinal Surgery, Nankai Hospital, Tianjin 300100, China
Chang-Lin Zou, Graduate School of Tianjin Medical University, Tianjin 300100, China

Dong-Hua Li, Tianjin Institute of Acute Abdominal Diseases of Integrated Traditional Chinese and Western Medicine, Tianjin 300100, China

Nai-Qiang Cui, Department of Hepatopancreatobiliary Surgery, Nankai Hospital, Tianjin 300100, China

Author contributions: Yu XY and Zou CL contributed equally to this study and performed the majority of the experiments; Zhou ZL, Shan T and Li DH participated in the performance of experiments; Yu XY and Cui NQ designed the study and wrote the manuscript.

Supported by National Program on Key Basic Research Project, No. 2009CB522703

Correspondence to: Xiang-Yang Yu, MD, Department of Gastrointestinal Surgery, Nankai Hospital, Nankai District, No. 6 Changjiang Rd, Tianjin 300100, China. yxynankai@126.com
Telephone: +86-22-27435860 Fax: +86-22-27435860

Received: September 3, 2013 Revised: February 21, 2014

Accepted: April 1, 2014

Published online: July 7, 2014

Abstract

AIM: To investigate the phasic alteration of intestinal homeostasis in an experimental model of intestinal obstruction.

METHODS: A rabbit model of intestinal obstruction was established by transforming parts of an infusion set into an *in vivo* pulled-type locking clamp and creating a uniform controllable loop obstruction in the mesenteric non-vascular zone 8 cm from the distal end of the ileum. The phasic alteration of intestinal homeostasis was studied after intestinal obstruction. The changes in goblet cells, intraepithelial lymphocytes, lamina propria lymphocytes, and intestinal epithelium were quantified from periodic acid-Schiff-stained sections. Ornithine decarboxylase (ODC) activity and serum citrulline levels were measured by high-performance

liquid chromatography. Claudin 1 mRNA expression was examined by real-time polymerase chain reaction analysis. Intestinal microorganisms, wet/dry weight ratios, pH values, and endotoxin levels were determined at multiple points after intestinal obstruction. Furthermore, the number and ratio of CD3⁺, CD4⁺ and CD8⁺ T cells were determined by flow cytometry, and secretory IgA levels were measured with an enzyme-linked immunosorbent assay.

RESULTS: A suitable controllable rabbit model of intestinal obstruction was established. Intestinal obstruction induced goblet cell damage and reduced cell number. Further indicators of epithelial cell damage were observed as reduced serum citrulline levels and claudin 1 gene expression, and a transient increase in ODC activity. In addition, the wet/dry weight ratio and pH of the intestinal lumen were also dramatically altered. The ratio of *Bacillus bifidus* and enterobacteria was reversed following intestinal obstruction. The number and area of Peyer's patches first increased then sharply decreased after the intestinal obstruction, along with an alteration in the ratio of CD4/CD8⁺ T cells, driven by an increase in CD3⁺ and CD8⁺ T cells and a decrease in CD4⁺ T cells. The number of lamina propria lymphocytes also gradually decreased with prolonged obstruction.

CONCLUSION: Intestinal obstruction can induce disruption of intestinal homeostasis.

© 2014 Baishideng Publishing Group Inc. All rights reserved.

Key words: Intestinal obstruction; Rabbit model; Homeostasis disruption; Intestinal epithelial cells; Intestinal microorganisms; Intestinal immune system

Core tip: A controllable rabbit model of intestinal obstruction was established. This model demonstrated that intestinal obstruction (1) induced intestinal epithelial cell damage and reduction; (2) disrupted the balance of intestinal microorganisms by abnormal pro-

liferation of pathogenic bacteria; and (3) disrupted the intestinal immune system, observed as a decrease in the number and area of Peyer's patches, and alteration of CD4⁺ T cell number and CD4/CD8⁺ T cell ratio. Furthermore, the levels of ornithine decarboxylase activity and citrulline and claudin 1 expression could serve as indicators of intestinal epithelial cell damage.

Yu XY, Zou CL, Zhou ZL, Shan T, Li DH, Cui NQ. Phasic study of intestinal homeostasis disruption in experimental intestinal obstruction. *World J Gastroenterol* 2014; 20(25): 8130-8138 Available from: URL: <http://www.wjgnet.com/1007-9327/full/v20/i25/8130.htm> DOI: <http://dx.doi.org/10.3748/wjg.v20.i25.8130>

INTRODUCTION

Intestinal obstruction is a common complication in abdominal surgery with significant morbidity and mortality rates^[1]. The most common causes of intestinal obstruction include intra-abdominal adhesions, intestinal herniation, gut strangulation, and abdominal tumors. The clinical symptoms include nausea and emesis, colicky abdominal pain, and a failure to pass flatus or bowel movements^[2]. Models of intestinal obstruction, such as in mice, rats, rabbits, and pigs^[3-6], are important tools for investigating the pathogenic mechanisms of intestinal obstruction. However, there is no well-established model that accurately reconstructs the complex symptoms of human intestinal obstruction. Therefore, it is necessary to establish a good experimental model to study the effects of intestinal obstruction.

As the most common cause for abdominal emergency, the major concerns of intestinal obstruction are its effects on whole body fluid and electrolyte balances and the mechanical effect on intestinal perfusion^[7]. However, the precise role of intestinal obstruction in the disruption of intestinal homeostasis, which depends on complex interactions between the intestinal epithelium, microorganisms and the intestinal immune system^[8,9], is not entirely clear. These interactions are also important for the pathogenesis of intestinal disorders other than intestinal obstruction^[10], such as inflammatory bowel disease^[11] and Crohn's disease^[12].

However, to the best of our knowledge, no relevant studies to date have focused on the alteration of intestinal homeostasis in experimental intestinal obstruction. In the current study, a controllable rabbit model of intestinal obstruction was established and used to evaluate the effects of intestinal obstruction on damage and recovery of intestinal epithelial cells, and on the intestinal microorganisms and immune system.

MATERIALS AND METHODS

Animals

Healthy New Zealand rabbits weighing 2.5-3.0 kg were

purchased from the Mingle Laboratory Animal Center (Tianjin, China) and maintained in a temperature-controlled room with 12-h light/dark cycles and access to regular chow and water. The experimental procedures were approved by the Laboratory Animal Care Committee at Tianjin Medical University.

Establishment of rabbit intestinal obstruction model

Forty-eight rabbits were randomly divided into eight experimental groups ($n = 6$ per group). The experimental protocols were carried out under aseptic conditions. Animals were anesthetized with urethane (intravenous delivery; 1 g/kg) and a laparotomy was performed. A uniform controllable loop obstruction was created by placing a clamp in the mesenteric non-vascular zone, 8 cm from the distal end of the ileum. The animals were allowed to recover postoperatively for 3 d, after which the clamp was locked (indicated by the green color label), resulting in obstruction of the intestine. Sham-operated rabbits received mock manipulation of the gut without locking of the clamp device. The experimental animals, nonoperated controls, and sham-operated controls were sacrificed for experiments at various times after obstruction (between 1 and 72 h).

Cell quantification

Intestinal segments 2 cm in length from the ileum (5 cm distal to the obstruction) were excised and fixed in 4% formaldehyde and embedded in paraffin blocks. Tissue was cut into 4- μ m-thick sections for periodic acid-Schiff (PAS) staining using standard protocols^[13]. The sections were examined and quantified using a Champion-500w graphic report management system (Beijing Kong Hai Science and Technology Development Co. Ltd., Beijing, China). The number, diameter and area of goblet cells (GCs) were obtained from 25 villi per section and quantified as the number of cells/total area \times 10000. Intraepithelial lymphocytes (IELs) and lamina propria lymphocytes (LPLs) were similarly counted from 25 villi per section and expressed as a percentage of total cells.

HPLC analysis

Ornithine decarboxylase (ODC) activity of intestinal tissues and the serum level of citrulline were analyzed by HPLC as described previously^[14,15].

RNA extraction and real-time polymerase chain reaction

RNA was extracted from intestinal segments (100 mg) (5 cm distal to the obstruction) using the Total RNA Kit (Qiagen, Venlo, Limburg, Netherlands), following the manufacturer's instructions. First-strand cDNA was synthesized from 1 μ g mRNA using reverse transcriptase (Fermentas, Glen Burnie, MD, United States) and oligo (dT) primers. Real-time PCR was performed with an Applied Biosystems PRISM 7300 system using SYBR Green polymerase chain reaction (PCR) Master Mix (Applied Biosystems by Life Technologies/Thermo Fisher

Scientific, Waltham, MA, USA) for claudin 1 (forward: 5'-GTGCCTTGATGGTGAATTG-3', reverse: 5'-AAAGTAGCCAGACCT GAAAT-3') and normalized to β -actin (forward: 5'-TGATGGTGGGCATGGGTC-3', reverse: 5'-CGATGGGGTACTTCAGGGTG-3').

Detection of luminal microorganisms

The intestinal contents were obtained from the ileum (5 cm distal to the obstruction) and weighed. Samples of intestinal content (200 mg) were diluted 10-fold and then plated on fresh eosin methylene blue or trypticase-peptone-yeast selective culture medium plates and cultured for 48 h at 37 °C. The number of bacteria was calculated as colony-forming units per g (log CFU/g).

Measurement of ileum wet/dry ratio and pH value

For measurement of ileum wet/dry ratio^[4], the intestinal contents from a 5-cm intestinal segment (5 cm distal to the obstruction) were weighed (wet weight value) and the segment was then dried by baking, after which the dry weight was recorded. The pH of the intestinal lumen was measured with medical pH indicator paper.

Limulus amebocyte lysate assay

To determine the endotoxin concentration in serum at different times after intestinal obstruction, an Limulus amebocyte lysate (LAL) assay was performed using a commercial kit according to the manufacturer's protocol (Chinese Horseshoe Crab Reagent Manufactory, Xiamen, China). Serum samples were collected and analyzed using pyrogen-free materials, diluted 10% (v/v) in LAL reagent water, and heated to 70 °C for 5 min to remove any non-specific inhibition. Samples were then incubated with equal volumes of LAL for 10 min at 37 °C and developed with equal volumes of substrate solution for 6 min. The absorbance of the assay plate was read at 545 nm using a microplate reader (BioTek, Winooski, VT, United States).

Flow cytometry analysis of Peyer's patch lymphocytes

Peyer's patch (PP) lymphocytes were isolated as described previously^[16]. PPs were excised and incubated in sterile conditions in RPMI medium containing 1 mmol/L dithiothreitol for 5 min at 37 °C. Thereafter, the PPs were washed with RPMI medium and passed through a steel mesh. The resultant cell suspension was washed and resuspended in RPMI containing 10% fetal bovine serum. The PP lymphocytes were incubated at 4 °C for 30 min with fluorescein-isothiocyanate-conjugated anti-rabbit CD4, phycoerythrin-conjugated anti-rabbit CD8 and PerCP-Cy5.5-conjugated anti-rabbit CD3 antibodies (Antigenix, Huntington Station, NY, United States). Negative controls were stained with isotype-matched monoclonal antibodies. Cells were washed and resuspended in phosphate-buffered saline (PBS) for fluorescence-activated cell sorting (FACS) analysis. Data were acquired with a FACS Calibur flow cytometer and analyzed using Cell Quest software (BD Biosciences, Franklin Lakes, NJ, United States).

Measurement of IgA level by enzyme-linked immunosorbent assay

Extracts for enzyme-linked immunosorbent assay (ELISA) analysis were obtained by flushing 3 mL sterile PBS through an 8-cm intestinal segment (5 cm distal to the obstruction) with the solid intestinal contents removed. The obtained extracts were centrifuged and the supernatants were collected. The levels of secretory IgA (s-IgA) were measured using an ELISA kit (USCN Life Science, Wuhan, China) according to the manufacturer's instructions.

Statistical analysis

The software package SPSS version 17.0 (SPSS, Chicago, IL, United States) was used for statistical analyses. One-way analysis of variance was used for comparing values obtained in three or more groups. Frequency variables were compared using the χ^2 test. Data are expressed as mean \pm SD and $P < 0.05$ was regarded as statistically significant.

RESULTS

Modified and controllable rabbit model of intestinal obstruction

A controllable intestinal obstruction model was developed in the rabbit by using the intestinal extrinsic oppressive method. Infusion set parts that are widely used in clinical settings were transformed into an *in vivo* pulled-type locking clamp (Figure 1A). After laparotomy, a uniform controllable loop obstruction was created with a clamp in the mesenteric non-vascular zone placed 8 cm from the distal end of the ileum (Figure 1B). Three days after the operation, the clamp was locked, resulting in the obstruction of the intestine. Obstruction resulted in a gross pathological changes observed as bowel distension, hyperemia edema, cyanosis, adhesions, perforation, free peritoneal fluid, or even enteroparalysis, which became more apparent with extended obstruction time (Figure 1C, D).

Effect of intestinal obstruction on intestinal epithelial cells

Experimental animals, non-operated controls, and sham-operated controls were sacrificed at various times after intestinal obstruction (between 1 and 72 h). Quantification of GC number, diameter and area from PAS-stained tissue sections demonstrated that there was an increase in the number of GCs 48 h after obstruction (Figure 2A). The diameter and area of GCs initially decreased during the first 12 h of obstruction and then recovered by 72 h (Figure 2B, D). Evidence suggesting a proliferation of intestinal epithelial cells was supported by changes in the activity of ODC, which increased after obstruction and peaked at 12 h, then rapidly decreased (Figure 2E). However, the number of GCs dramatically decreased after 48 h, paralleled by a decrease in blood citrulline levels after 24 h (Figure 2F), indicating severe damage in the intestinal epithelium and the shedding of cells (Figure 2C). Furthermore, expression of claudin 1 mRNA, encoding a protein involved in the formation of

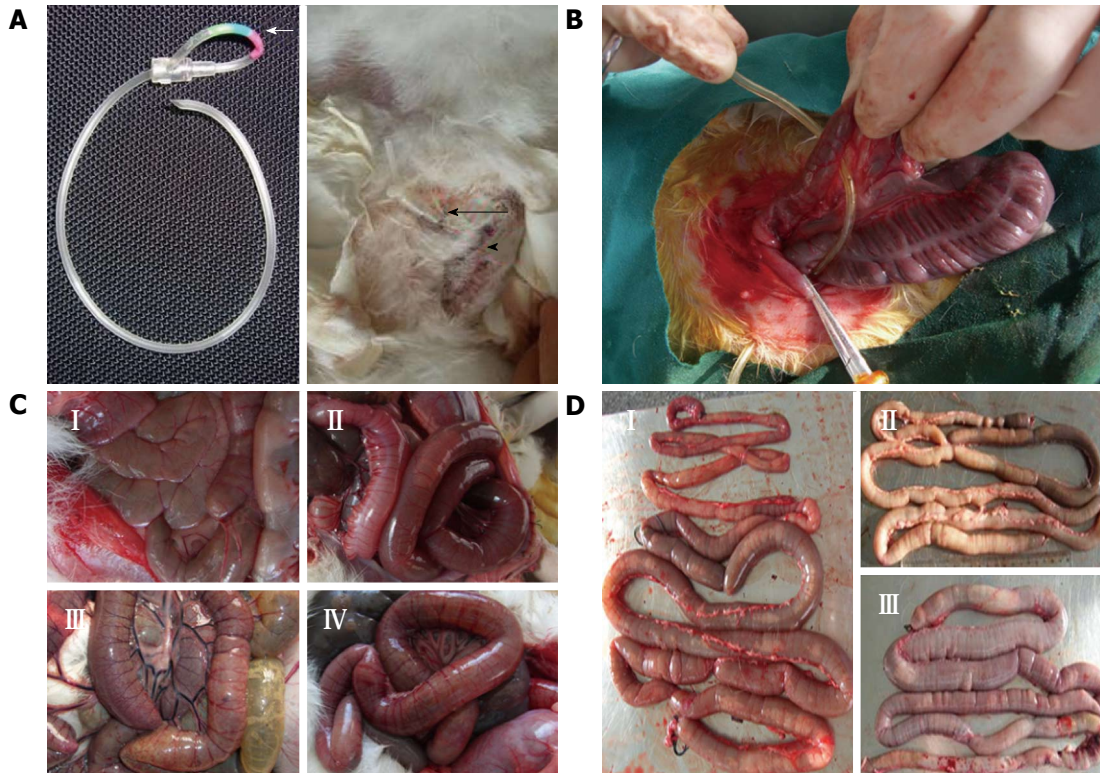


Figure 1 Establishment of a modified and controllable rabbit model of intestinal obstruction. A: The infusion set used in this study (left), the color labels indicating the status of the lock, (right) the cut after saturation; B: Assembling the *in vivo* pulled-type locking clamp; C: Effect of obstruction for (I) sham-operated control and at (II) 24 h, (III) 48 h, and (IV) 72 h after obstruction; D: Gross morphology of intestinal obstruction at (I) 24 h, (II) 48 h, and (III) 72 h after obstruction.

epithelial tight junctions, was significantly reduced 6 h after obstruction ($P < 0.05$) and almost undetectable at 72 h.

Effect of intestinal obstruction on intestinal microorganisms

Two types of intestinal bacteria were examined after intestinal obstruction. Following obstruction, the amount of *Bacillus bifidus* gradually decreased and enterobacteria increased such that by 24 h after obstruction, a reversal of their ratios was observed, with enterobacteria progressively becoming the dominant bacteria in the intestinal lumen (Figure 3A, B). In addition, the wet/dry weight ratio of intestinal contents and the pH value of intestinal lumen were also dramatically altered (Figure 3C). An LAL assay demonstrated that the concentration of endotoxins produced by pathogenic bacteria dramatically increased with prolonged obstruction (Figure 3D).

Effect of intestinal obstruction on intestinal immune system

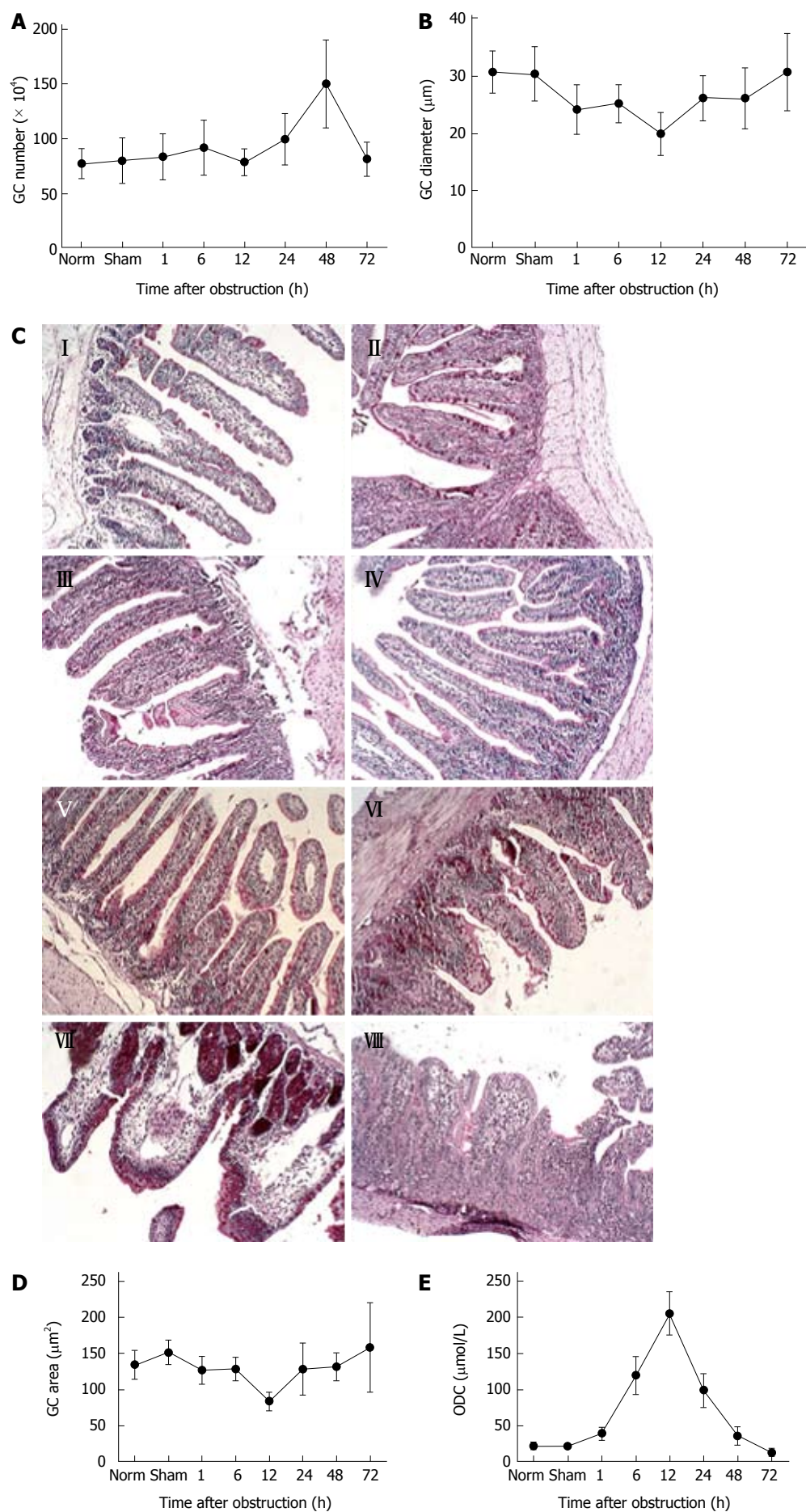
An analysis of PPs indicated that intestinal obstruction resulted in an initial increase in their number and size from 1 to 24 h after obstruction, followed by a sharp decrease from 24 to 72 h (Figure 4A, B). FACS analysis revealed an increase in CD3⁺ and CD8⁺ T cells at 48 and 72 h post-obstruction, accompanied by a decrease in CD4⁺ T cells (Figure 4C-E). As a result, the CD4/CD8 ratio first increased (1-24 h), then sharply declined with

prolonged obstruction (24-72 h) (Figure 4F). There was also a trend towards a decrease in the amount of s-IgA with time from obstruction, although this difference was not significant (Figure 4G). Furthermore, the data showed that there was no significant difference found in the number of IELs during obstruction (Figure 4H), while the number of LPLs gradually decreased with the duration of obstruction (Figure 4I).

DISCUSSION

Intestinal obstruction of the small or large intestines induces a series of changes in the obstructed segments that cause symptoms, such as bloating, vomiting, abdominal cramps and constipation, and can lead to intestinal failure^[17,18]. Although the functional and morphological changes have been well documented in the literature, the role of intestinal obstruction in the disruption of intestinal homeostasis is not fully understood. Current established animal models of complete intestinal obstruction are not controllable^[19], therefore, a new animal model was developed and used to examine the effects of complete obstruction. Our results provide evidence for a robust relationship between intestinal homeostasis and obstruction.

A controllable rabbit model of intestinal obstruction was established by transforming infusion set parts widely used in clinics into an *in vivo* pulled-type locking clamp. The clamp was placed 8 cm from the distal



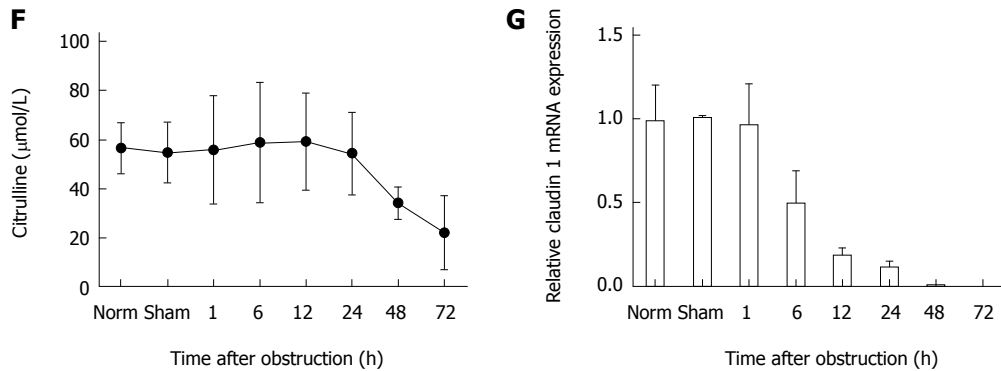


Figure 2 Intestinal obstruction alters intestinal epithelial cells. A: Number; B: Diameter; and D: Area of goblet cells (GCs) in obstructed ileum; C: Periodic acid-Schiff-stained intestinal tissue sections from (I) non-operated controls, (II) sham-operated controls and at (III) 1 h, (IV) 6 h, (V) 12 h, (VI) 24 h, (VII) 48 h and (VIII) 72 h after obstruction; E: Ornithine decarboxylase (ODC) activity in intestinal tissues; F: Level of citrulline in serum; G: Claudin 1 gene expression.

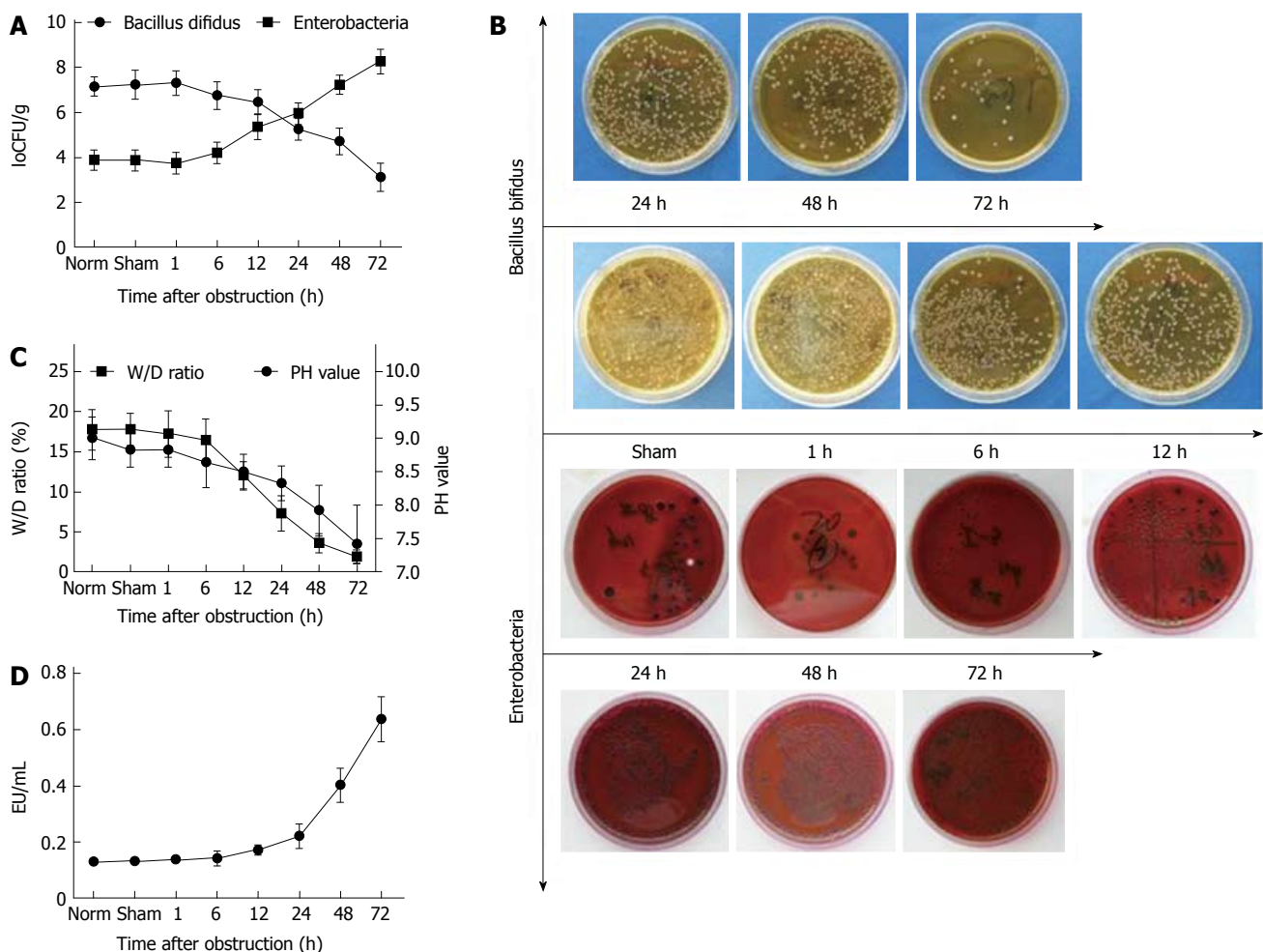


Figure 3 Intestinal obstruction disrupts the balance of intestinal microorganisms. Quantification of A: *Bacillus bifidus* and B: enterobacteria in the intestinal lumen; C: Wet/dry weight ratio for intestinal contents and pH value of intestinal lumen; D: Serum endotoxin levels.

end of the ileum to create a uniform controllable loop obstruction. This method has several advantages compared to previously described rabbit models because it involves a faster surgical procedure, reduced trauma, and the use of more cost-effective materials, as well as minimizing the risk of intra-abdominal infection, and intestinal adhesions and perforation^[5,20]. It replicates the

complex symptoms of human intestinal obstruction, with effects evident after prolonged obstruction. Within 72 h, the intestinal epithelia was found to be severely damaged, with a dramatic decrease in GC number after 48 h. Epithelial damage can be observed as changes in levels of ODC^[21] and blood citrulline^[22], which were both dramatically decreased by obstruction in our model,

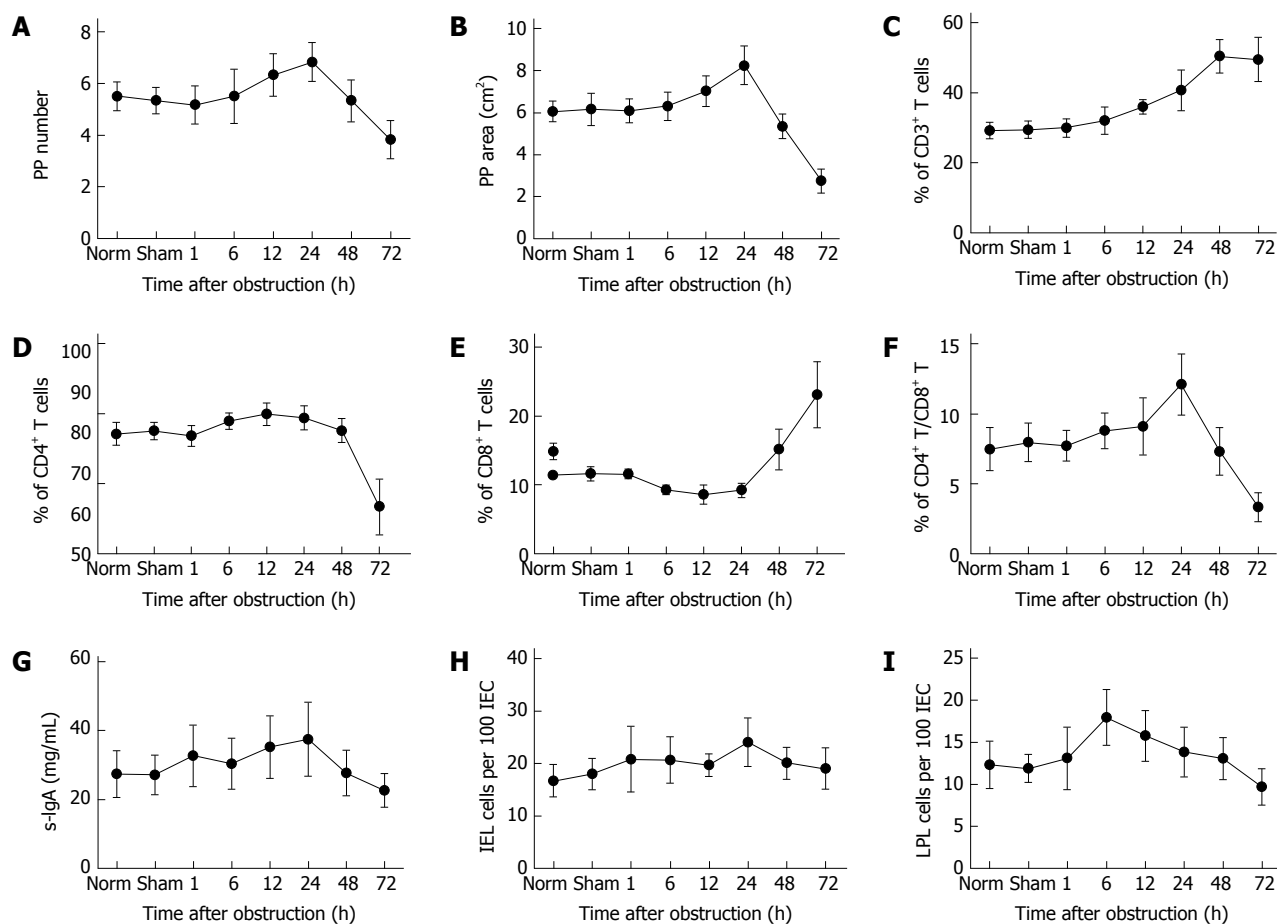


Figure 4 Intestinal obstruction disrupts the intestinal immune system. A: The number; B: area of Peyer's patch (PP) in obstructed ileum quantified from periodic acid-Schiff-stained tissue sections; Percentages of C: CD3⁺ T cells; D: CD4⁺ T cells; E: CD8⁺ T cells; F: Ratio of CD4⁺/CD8⁺ T cells; G: The level of s-IgA in intestinal lumen; H: Quantification of intraepithelial lymphocytes (IELs); I: Quantification of lamina propria lymphocytes (LPLs).

indicating an imbalance of damage and recovery of intestinal epithelia. The intestinal epithelial integrity was completely lost with prolonged obstruction, and the intestinal mechanical barrier was severely compromised, as indicated by the decrease in expression of claudin 1; a transmembrane component of tight junctions between intestinal epithelial cells^[23,24]. These junctions constitute continuous, circumferential seals around cells that serve as a physical barrier^[23]. These findings suggest that an imbalance between intestinal epithelial cell damage and recovery occurs with prolonged obstruction. Furthermore, the data suggest that levels of ODC and citrulline combined with claudin 1 expression could serve as indicators of the degree of intestinal epithelial cell damage after intestinal obstruction.

The intestinal lumen hosts a large amount of commensal bacteria^[26], and a large body of evidence has now confirmed the important role of these microbes in the maintenance of intestinal homeostasis^[27-29]. This homeostasis, which involves intestinal epithelial cells, luminal microorganisms and gut-associated lymphoid tissue^[30], is initially disrupted following intestinal obstruction. Damage to intestinal epithelial cells can lead to an alteration of luminal microorganisms^[31], including commensal bacteria, such as *Bacillus bifidus*, and pathogenic bacteria,

such as *Enterobacteriaceae*^[32]. The ratio of these two types of bacteria was inverted following obstruction, corresponding to an increase in serum endotoxin. In addition, there was a decrease in the wet/dry weight ratio and luminal pH, suggesting that this alteration in the balance of intestinal microorganisms disrupted the internal milieu of the intestine.

Equilibrium between the microbiota and the intestinal immune system is fundamental to intestinal homeostasis. Excessive and constitutive activation of immune responses can cause gut tissue destruction, thus, a response is mounted by intestinal immune cells in order to maintain intestinal homeostasis^[33]. The gut-associated lymphoid tissue consists of secondary lymphoid organs including PPs, mesenteric lymph nodes, IELs, and LPLs^[34]. In this study, complete intestinal obstruction resulted in an initial increase in the number and area of PPs, followed by a sharp decline. The number of LPLs also declined with obstruction. Furthermore, the percentages of T cell subtypes in PP lymphocytes were altered, indicating that the intestinal obstruction disrupted the intestinal immune system.

In summary, the data demonstrate the use of a novel model of intestinal obstruction that results in a disruption of intestinal homeostasis. However, further studies

are needed to determine the precise mechanism of this disruption. The findings of the present study suggest that restoration of intestinal homeostasis would provide a viable therapeutic target for treatment of intestinal obstruction.

COMMENTS

Background

Intestinal obstruction is a common complication from abdominal surgery, with significant morbidity and mortality rates. Although there are several animal models for studying intestinal obstruction, there is no well-established model that reflects the complex symptoms that occur with intestinal obstruction in humans. A more relevant animal model is therefore needed to investigate the pathogenic processes that occur with intestinal obstruction.

Research frontiers

Although the functional and morphological changes from intestinal obstruction have been well documented in the literature, the role of intestinal obstruction in the disruption of intestinal homeostasis is not well defined. Intestinal homeostasis depends on complex interactions between the intestinal epithelium, microorganisms and immune system. To date, there are no relevant studies focused on the alteration of intestinal homeostasis in experimental intestinal obstruction.

Innovations and breakthroughs

The present study establishes the use of a controllable rabbit model of intestinal obstruction. By using this model, the authors have demonstrated that intestinal obstruction induces intestinal epithelial cell damage and loss and an imbalance of intestinal microorganisms resulting from the abnormal proliferation of pathogenic bacteria, as well as an alteration in the ratio of intestinal immune cell types.

Applications

These findings validate a novel model of intestinal obstruction, and suggest that restoration of intestinal homeostasis may be an attractive strategy for treatment of human intestinal obstruction.

Terminology

The intestinal microbiota refers to the tens of trillions of microorganisms, including commensal and pathogenic bacteria, living in the intestine. The gut-associated lymphoid tissue consists of secondary lymphoid organs including Peyer's patches, mesenteric lymph nodes, intraepithelial lymphocytes, and lamina propria lymphocytes. Ornithine decarboxylase levels indicate the proliferative ability of intestinal epithelial cells. IgA is the predominant antibody isotype in intestinal fluid, which protect against a variety of foreign antigens. The transmembrane protein claudin 1 is a functional component of intestinal epithelial cell tight junctions.

Peer review

The authors established a novel animal model to investigate the effects of intestinal obstruction. Results revealed a strong association between intestinal obstruction and disruption of intestinal homeostasis. However, further study is needed to determine the precise mechanism of homeostatic disruption following intestinal obstruction.

REFERENCES

- Cappell MS, Batke M. Mechanical obstruction of the small bowel and colon. *Med Clin North Am* 2008; **92**: 575-597, viii [PMID: 18387377 DOI: 10.1016/j.mcna.2008.01.003]
- Zielinski MD, Bannon MP. Current management of small bowel obstruction. *Adv Surg* 2011; **45**: 1-29 [PMID: 21954676]
- Chang IY, Glasgow NJ, Takayama I, Horiguchi K, Sanders KM, Ward SM. Loss of interstitial cells of Cajal and development of electrical dysfunction in murine small bowel obstruction. *J Physiol* 2001; **536**: 555-568 [PMID: 11600689]
- Yuan ML, Yang Z, Li YC, Shi LL, Guo JL, Huang YQ, Kang X, Cheng JJ, Chen Y, Yu T, Cao DQ, Pang H, Zhang X. Comparison of different methods of intestinal obstruction in a rat model. *World J Gastroenterol* 2013; **19**: 692-705 [PMID: 23430052 DOI: 10.3748/wjg.v19.i5.692]
- Mulvihill SJ, Pappas TN, Fonkalsrud EW, Debas HT. The effect of somatostatin on experimental intestinal obstruction. *Ann Surg* 1988; **207**: 169-173 [PMID: 2893593]
- Collins J, Vicente Y, Georgeson K, Kelly D. Partial intestinal obstruction induces substantial mucosal proliferation in the pig. *J Pediatr Surg* 1996; **31**: 415-419 [PMID: 8708915]
- Jackson PG, Raiji MT. Evaluation and management of intestinal obstruction. *Am Fam Physician* 2011; **83**: 159-165 [PMID: 21243991]
- Artis D. Epithelial-cell recognition of commensal bacteria and maintenance of immune homeostasis in the gut. *Nat Rev Immunol* 2008; **8**: 411-420 [PMID: 18469830 DOI: 10.1038/nri2316]
- Hooper LV, Macpherson AJ. Immune adaptations that maintain homeostasis with the intestinal microbiota. *Nat Rev Immunol* 2010; **10**: 159-169 [PMID: 20182457 DOI: 10.1038/nri2710]
- DuPont AW, DuPont HL. The intestinal microbiota and chronic disorders of the gut. *Nat Rev Gastroenterol Hepatol* 2011; **8**: 523-531 [PMID: 21844910 DOI: 10.1038/nrgastro.2011.133]
- Maloy KJ, Powrie F. Intestinal homeostasis and its breakdown in inflammatory bowel disease. *Nature* 2011; **474**: 298-306 [PMID: 21677746 DOI: 10.1038/nature10208]
- Jiang W, Wang X, Zeng B, Liu L, Tardivel A, Wei H, Han J, MacDonald HR, Tschopp J, Tian Z, Zhou R. Recognition of gut microbiota by NOD2 is essential for the homeostasis of intestinal intraepithelial lymphocytes. *J Exp Med* 2013; **210**: 2465-2476 [PMID: 24062413 DOI: 10.1084/jem.20122490]
- McDole JR, Wheeler LW, McDonald KG, Wang B, Konjufca V, Knoop KA, Newberry RD, Miller MJ. Goblet cells deliver luminal antigen to CD103+ dendritic cells in the small intestine. *Nature* 2012; **483**: 345-349 [PMID: 22422267 DOI: 10.1038/nature10863]
- Escribano MI, Legaz ME. High performance liquid chromatography of the dansyl derivatives of putrescine, spermidine, and spermine. *Plant Physiol* 1988; **87**: 519-522 [PMID: 16666175]
- Bai C, Reilly CC, Wood BW. Identification and quantitation of asparagine and citrulline using high-performance liquid chromatography (HPLC). *Anal Chem Insights* 2007; **2**: 31-36 [PMID: 19662174]
- Ramiro-Puig E, Pérez-Cano FJ, Ramos-Romero S, Pérez-Berzeto T, Castellote C, Permanyer J, Franch A, Izquierdo-Pulido M, Castell M. Intestinal immune system of young rats influenced by cocoa-enriched diet. *J Nutr Biochem* 2008; **19**: 555-565 [PMID: 18061430 DOI: 10.1016/j.jnutbio.2007.07.002]
- Prihoda M, Flatt A, Summers RW. Mechanisms of motility changes during acute intestinal obstruction in the dog. *Am J Physiol* 1984; **247**: G37-G42 [PMID: 6742196]
- Thompson JS. Overview of etiology and management of intestinal failure. *Gastroenterology* 2006; **130**: S3-S4 [PMID: 16473069 DOI: 10.1053/j.gastro.2005.09.062]
- Attard JA, MacLean AR. Adhesive small bowel obstruction: epidemiology, biology and prevention. *Can J Surg* 2007; **50**: 291-300 [PMID: 17897517]
- Kurzbauer R. [Improved experimental model of ileus of the small intestine in the rabbit and its use for measuring the duration of postoperative intestinal paralysis]. *Pol Przegl Chir* 1977; **49**: 419-423 [PMID: 859776]
- Pendeville H, Carpino N, Marine JC, Takahashi Y, Muller M, Martial JA, Cleveland JL. The ornithine decarboxylase gene is essential for cell survival during early murine development. *Mol Cell Biol* 2001; **21**: 6549-6558 [PMID: 11533243]
- Crenn P, Coudray-Lucas C, Cynober L, Messing B. Post-absorptive plasma citrulline concentration: a marker of intestinal failure in humans. *Transplant Proc* 1998; **30**: 2528 [PMID: 9745471]
- Singh AB, Sharma A, Dhawan P. Claudin family of proteins and cancer: an overview. *J Oncol* 2010; **2010**: 541957 [PMID: 20671913 DOI: 10.1155/2010/541957]
- Günzel D, Fromm M. Claudins and other tight junction proteins. *Compr Physiol* 2012; **2**: 1819-1852 [PMID: 23723025]

- DOI: 10.1002/cphy.c110045]
- 25 **Zuhl M**, Schneider S, Lanphere K, Conn C, Dokladny K, Moseley P. Exercise regulation of intestinal tight junction proteins. *Br J Sports Med* 2014; **48**: 980-986 [PMID: 23134759 DOI: 10.1136/bjsports-2012-091585]
 - 26 **Bäckhed F**, Ley RE, Sonnenburg JL, Peterson DA, Gordon JI. Host-bacterial mutualism in the human intestine. *Science* 2005; **307**: 1915-1920 [PMID: 15790844 DOI: 10.1126/science.1104816]
 - 27 **Tanoue T**, Umesaki Y, Honda K. Immune responses to gut microbiota-commensals and pathogens. *Gut Microbes* 2010; **1**: 224-233 [PMID: 21327029 DOI: 10.4161/gmic.1.4.12613]
 - 28 **Maslowski KM**, Mackay CR. Diet, gut microbiota and immune responses. *Nat Immunol* 2011; **12**: 5-9 [PMID: 21169997 DOI: 10.1038/ni0111-5]
 - 29 **Duerkop BA**, Vaishnava S, Hooper LV. Immune responses to the microbiota at the intestinal mucosal surface. *Immunity* 2009; **31**: 368-376 [PMID: 19766080 DOI: 10.1016/j.immuni.2009.08.009]
 - 30 **Magrone T**, Jirillo E. The interplay between the gut immune system and microbiota in health and disease: nutraceutical intervention for restoring intestinal homeostasis. *Curr Pharm Des* 2013; **19**: 1329-1342 [PMID: 23151182]
 - 31 **Ohland CL**, Macnaughton WK. Probiotic bacteria and intestinal epithelial barrier function. *Am J Physiol Gastrointest Liver Physiol* 2010; **298**: G807-G819 [PMID: 20299599 DOI: 10.1152/ajpgi.00243.2009]
 - 32 **Packey CD**, Sartor RB. Commensal bacteria, traditional and opportunistic pathogens, dysbiosis and bacterial killing in inflammatory bowel diseases. *Curr Opin Infect Dis* 2009; **22**: 292-301 [PMID: 19352175 DOI: 10.1097/QCO.0b013e32832a8a5d]
 - 33 **Round JL**, Mazmanian SK. The gut microbiota shapes intestinal immune responses during health and disease. *Nat Rev Immunol* 2009; **9**: 313-323 [PMID: 19343057 DOI: 10.1038/nri2515]
 - 34 **Forchielli ML**, Walker WA. The role of gut-associated lymphoid tissues and mucosal defence. *Br J Nutr* 2005; **93** Suppl 1: S41-S48 [PMID: 15877894]

P- Reviewers: Kate V, Shoaran M **S- Editor:** Gou SX
L- Editor: Kerr C **E- Editor:** Liu XM





Published by **Baishideng Publishing Group Inc**

8226 Regency Drive, Pleasanton, CA 94588, USA

Telephone: +1-925-223-8242

Fax: +1-925-223-8243

E-mail: bpgoffice@wjgnet.com

Help Desk: <http://www.wjgnet.com/esps/helpdesk.aspx>

<http://www.wjgnet.com>



ISSN 1007-9327

